

## 2. RECIPROCAL SPACE IN CRYSTAL-STRUCTURE DETERMINATION

determined to be  $10/mmm$ . Fig. 2.5.3.27(d) shows a CBED pattern taken by slightly tilting the incident beam to the  $c^*$  direction from incidence A. Dynamical extinction lines (arrowheads) are seen in the odd-order reflections along the  $c^*$  axis. This indicates the existence of a  $10_5$  screw axis and a  $c$ -glide plane. No other reflection absences were observed, implying the lattice type to be primitive. Therefore, the space group of  $\text{Al}_{70}\text{Ni}_{20}\text{Fe}_{10}$  is determined to be centrosymmetric  $P10_5/mmc$ . It was found that the alloys with  $0 \leq x \leq 7.5$  belong to the noncentrosymmetric space group  $P\bar{1}0m2$  and those with  $7.5 < x \leq 15$  belong to the centrosymmetric space group  $P10_5/mmc$ , keeping the specific polar structure of the basic clusters unchanged.

Another phase was found in the same alloys with  $15 < x \leq 17$ . This phase showed the same CBED symmetries as the phase with  $7.5 < x \leq 15$ . The space group of the phase was also determined to be  $P10_5/mmc$ . However, high-angle annular dark-field (HAADF) observations of the phase with  $15 < x \leq 17$  showed that each atom cluster has only one mirror plane of symmetry (Saitoh *et al.*, 1997, 1999). This implies that the structure of the specific cluster is changed from that of the phase with  $7.5 < x \leq 15$ . The clusters are still polar but take ten different orientations, producing centrosymmetric tenfold rotation symmetry on average, which was confirmed by HAADF observations (Saitoh, Tanaka & Tsai, 2001).

These three phases have been found for the similar alloys  $\text{Al}-M1-M2$ , where  $M1 = \text{Ni}$  and  $\text{Cu}$ , and  $M2 = \text{Fe}$ ,  $\text{Co}$ ,  $\text{Rh}$  and  $\text{Ir}$  (Tanaka *et al.*, 1996). Subsequently, decagonal quasicrystals were found in  $\text{Al}-\text{Pd}-\text{Mn}$ ,  $\text{Zn}-\text{Mg}-\text{RE}$  ( $\text{RE} = \text{Dy}$ ,  $\text{Er}$ ,  $\text{Ho}$ ,  $\text{Lu}$ ,  $\text{Tm}$  and  $\text{Y}$ ) and other alloy systems (Steurer, 2004). There are seven point groups in the decagonal system (Table 2.5.3.15). However, only two point groups,  $\bar{1}0m2$  and  $10/mmm$ , and two space groups,  $P\bar{1}0m2$  and  $P10_5/mmc$ , are known reliably in real materials to date, though a few other point and space groups have been reported.

For further crystallographic aspects of quasicrystals, the reader is referred to the comprehensive reviews of Tsai (2003) and Steurer (2004), and to a review of more theoretical aspects by Yamamoto (1996).

**2.5.4. Electron-diffraction structure analysis (EDSA)<sup>2</sup>**

BY B. K. VAINSHTEIN AND B. B. ZVYAGIN

**2.5.4.1. Introduction**

Electron-diffraction structure analysis (EDSA) (Vainshtein, 1964) based on electron diffraction (Pinsker, 1953) is used for the investigation of the atomic structure of matter together with X-ray and neutron diffraction analysis. The peculiarities of EDSA, as compared with X-ray structure analysis, are defined by a strong interaction of electrons with the substance and by a short wavelength  $\lambda$ . According to the Schrödinger equation (see Section 5.2.2) the electrons are scattered by the electrostatic field of an object. The values of the atomic scattering amplitudes,  $f_e$ , are three orders higher than those of X-rays,  $f_x$ , and neutrons,  $f_n$ . Therefore, a very small quantity of a substance is sufficient to obtain a diffraction pattern. EDSA is used for the investigation of very thin single-crystal films, of  $\sim 5$ – $50$  nm polycrystalline and textured films, and of deposits of finely grained materials and surface layers of bulk specimens. The structures of many ionic crystals, crystal hydrates and hydro-oxides, various inorganic, organic, semiconducting and metallo-organic compounds, of various minerals, especially layer silicates, and of biological structures have been investigated by means of EDSA; it has also been used in the study of polymers, amorphous solids and liquids.

<sup>2</sup> Questions related to this section may be addressed to Dr D. L. Dorset (see list of contributing authors).

Special areas of EDSA application are: determination of unit cells; establishing orientational and other geometrical relationships between related crystalline phases; phase analysis on the basis of  $d_{hkl}$  and  $I_{hkl}$  sets; analysis of the distribution of crystallite dimensions in a specimen and inner strains in crystallites as determined from line profiles; investigation of the surface structure of single crystals; structure analysis of crystals, including atomic position determination; precise determination of lattice potential distribution and chemical bonds between atoms; and investigation of crystals of biological origin in combination with electron microscopy (Vainshtein, 1964; Pinsker, 1953; Zvyagin, 1967; Pinsker *et al.*, 1981; Dorset, 1976; Zvyagin *et al.*, 1979).

There are different kinds of electron diffraction (ED) depending on the experimental conditions: high-energy (HEED) (above 30–200 kV), low-energy (LEED) (10–600 V), transmission (THEED) and reflection (RHEED). In electron-diffraction studies use is made of special apparatus – electron-diffraction cameras in which the lens system located between the electron source and the specimen forms the primary electron beam, and the diffracted beams reach the detector without aberration distortions. In this case, high-resolution electron diffraction (HRED) is obtained. ED patterns may also be observed in electron microscopes by a selected-area method (SAD). Other types of electron diffraction are: MBD (microbeam), HDD (high-dispersion), CBD (convergent-beam), SMBD (scanning-beam) and RMBD (rocking-beam) diffraction (see Sections 2.5.2 and 2.5.3). The recent development of electron diffractometry, based on direct intensity registration and measurement by scanning the diffraction pattern against a fixed detector (scintillator followed by photomultiplier), presents a new improved level of EDSA which provides higher precision and reliability of structural data (Avilov *et al.*, 1999; Tsipursky & Drits, 1977; Zhukhlistov *et al.*, 1997, 1998; Zvyagin *et al.*, 1996).

Electron-diffraction studies of the structure of molecules in vapours and gases is a large special field of research (Vilkov *et al.*, 1978). See also *Stereochemical Applications of Gas-Phase Electron Diffraction* (1988).

**2.5.4.2. The geometry of ED patterns**

In HEED, the electron wavelength  $\lambda$  is about  $0.05 \text{ \AA}$  or less. The Ewald sphere with radius  $\lambda^{-1}$  has a very small curvature and is approximated by a plane. The ED patterns are, therefore, considered as plane cross sections of the reciprocal lattice (RL) passing normal to the incident beam through the point 000, to scale  $L\lambda$  (Fig. 2.5.4.1). The basic formula is

$$r = |\mathbf{h}|L\lambda, \text{ or } rd = L\lambda, \quad (2.5.4.1)$$

where  $r$  is the distance from the pattern centre to the reflection,  $\mathbf{h}$  is the reciprocal-space vector,  $d$  is the appropriate interplanar distance and  $L$  is the specimen-to-screen distance. The deviation of the Ewald sphere from a plane at distance  $h$  from the origin of the coordinates is  $\delta_h = h^2\lambda/2$ . Owing to the small values of  $\lambda$  and to the rapid decrease of  $f_e$  depending on  $(\sin \theta)/\lambda$ , the diffracted beams are concentrated in a small angular interval ( $\leq 0.1$  rad).

*Single-crystal ED patterns* image one plane of the RL. They can be obtained from thin ideal crystalline plates, mosaic single-crystal films or, in the RHEED case, from the faces of bulk single crystals. Point ED patterns can be obtained more easily owing to the following factors: the small size of the crystals (increase in the dimension of RL nodes) and mosaicity – the small spread of crystallite orientations in a specimen (tangential tension of the RL nodes). The crystal system, the parameters of the unit cell and the Laue symmetry are determined from point ED patterns; the probable space group is found from extinctions. Point ED patterns may be used for intensity measurements if the kinematic



## 2. RECIPROCAL SPACE IN CRYSTAL-STRUCTURE DETERMINATION

spherical surface with the centre at the point 000; the oblique cross section of such bands produces reflections in the form of arcs. The main interference curves for texture patterns are ellipses imaging oblique plane cross sections of the cylinders  $hk$  (Fig. 2.5.4.3).

At the normal electron-beam incidence (tilting angle  $\varphi = 0^\circ$ ) the ED pattern represents a cross section of cylinders perpendicular to the axis  $c^*$ , i.e. a system of rings.

On tilting the specimen to an angle  $\varphi$  with respect to its normal position (usually  $\varphi \simeq 60^\circ$ ) the patterns image an oblique cross section of the cylindrical RL, and are called oblique-texture (OT) ED patterns. The ellipses ( $hk = \text{constant}$ ) and layer lines ( $l = \text{constant}$ ) for orthogonal lattices are the main characteristic lines of ED patterns along which the reflections are arranged. The shortcoming of oblique-texture ED patterns is the absence of reflections lying inside the cone formed by rotation of the straight line coming from the point 000 at an angle  $(90^\circ - \varphi)$  around the axis  $c^*$  and, in particular, of reflections  $00l$ . However, at  $\varphi \lesssim 60-70^\circ$  the set of reflections is usually sufficient for structural determination.

For unit-cell determination and reflection indexing the values  $d$  (i.e.  $|\mathbf{h}|$ ) are used, and the reflection positions defined by the ellipses  $hk$  to which they belong and the values  $\eta$  are considered. The periods  $a^*$ ,  $b^*$  are obtained directly from  $h_{100}$  and  $h_{010}$  values. The period  $c^*$ , if it is normal to the plane  $a^*b^*$  ( $\gamma^*$  being arbitrary), is calculated as

$$c^* = \eta/l = (h_{hkl}^2 - h_{hk0}^2)^{1/2}/l. \quad (2.5.4.5a)$$

For oblique-angled lattices

$$c^* = [(h_{l+l}^2 + h_{l-l}^2 - 2h_l^2)/2]^{1/2}/l. \quad (2.5.4.5b)$$

In the general case of oblique-angled lattices the coaxial cylinders  $hk$  have radii

$$b_{hk} = (1/\sin \gamma)[(h^2/a^2) + (k^2/b^2) - (2hk \cos \gamma/ab)]^{1/2} \quad (2.5.4.6)$$

and it is always possible to use the measured or calculated values  $b_{hk}$  in (2.5.4.5a) instead of  $h_{hk0}$ , since

$$\eta = (h_{hkl}^2 - b_{hk}^2)^{1/2}. \quad (2.5.4.7)$$

In OT patterns the  $b_{hk}$  and  $\eta$  values are represented by the lengths of the small axes of the ellipses  $B_{hk} = L\lambda b_{hk}$  and the distances of the reflections  $hkl$  from the line of small axes (equatorial line of the pattern)

$$D_{hkl} = L\lambda\eta/\sin \varphi = hp + ks + lq. \quad (2.5.4.8)$$

Analysis of the  $B_{hk}$  values gives  $a$ ,  $b$ ,  $\gamma$ , while  $p$ ,  $s$  and  $q$  are calculated from the  $D_{hkl}$  values. It is essential that the components of the normal projections  $c_n$  of the axis  $c$  on the plane  $ab$  measured in the units of  $a$  and  $b$  are

$$\begin{aligned} x_n &= (c/a)(\cos \beta - \cos \alpha \cos \gamma)/\sin^2 \gamma \\ &= -p/q, \\ y_n &= (c/b)(\cos \alpha - \cos \beta \cos \gamma)/\sin^2 \gamma \\ &= -s/q. \end{aligned} \quad (2.5.4.9)$$

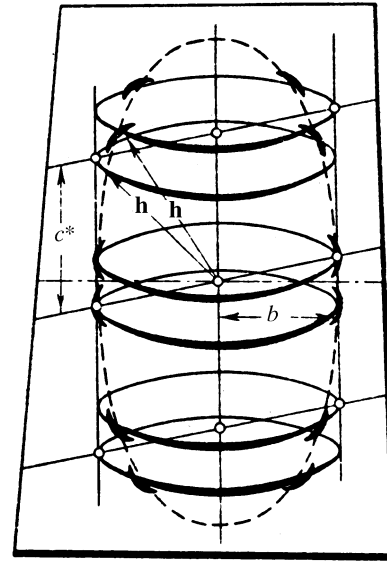


Fig. 2.5.4.3. Formation of ellipses on an electron-diffraction pattern from an oblique texture.

Obtaining  $x_n$ ,  $y_n$  one can calculate

$$c_n = [(x_n a)^2 + (y_n b)^2 + 2x_n y_n ab \cos \gamma]^{1/2}.$$

Since

$$\begin{aligned} d_{001} &= L\lambda/q \sin \varphi, \\ c &= (c_n^2 + d_{001}^2)^{1/2}. \end{aligned} \quad (2.5.4.10)$$

The  $\alpha$ ,  $\beta$  values are then defined by the relations

$$\begin{aligned} \cos \alpha &= (x_n a \cos \gamma + y_n b)/c, \\ \cos \beta &= (x_n a + y_n b \cos \gamma)/c. \end{aligned} \quad (2.5.4.11)$$

Because of the small particle dimensions in textured specimens, the kinematic approximation is more reliable for OT patterns, enabling a more precise calculation of the structure amplitudes from the intensities of reflections.

*Polycrystal ED patterns.* In this case, the RL is a set of concentric spheres with radii  $h_{hkl}$ . The ED pattern, like an X-ray powder pattern, is a set of rings with radii

$$r_{hkl} = h_{hkl}L\lambda. \quad (2.5.4.12)$$

### 2.5.4.3. Intensities of diffraction beams

The intensities of scattering by a crystal are determined by the scattering amplitudes of atoms in the crystal, given by (see also Section 5.2.1)

$$\begin{aligned} f_e^{\text{abs}}(s) &= 4\pi K \int \varphi(r)r^2 \frac{\sin sr}{sr} dr; \\ K &= \frac{2\pi m e}{h^2}; f_e = K^{-1}f_e^{\text{abs}}, \end{aligned} \quad (2.5.4.13)$$

where  $\varphi(r)$  is the potential of an atom and  $s = 4\pi(\sin \theta)/\lambda$ . The absolute values of  $f_e^{\text{abs}}$  have the dimensionality of length  $L$ . In EDSA it is convenient to use  $f_e$  without  $K$ . The dimensionality of